



Thiazole-5-carboxylic acid derivatives as potent xanthine oxidase inhibitors: design, synthesis, in vitro evaluation, and molecular modeling studies

Gurinder Kaur¹ · Jatinder V. Singh¹ · Manish K. Gupta² · Kavita Bhagat¹ · Harmandeep K. Gulati¹ · Atamjit Singh¹ · Preet Mohinder S. Bedi¹ · Harbinder Singh¹ · Sahil Sharma¹

Received: 14 December 2018 / Accepted: 14 October 2019
© Springer Science+Business Media, LLC, part of Springer Nature 2019

Abstract

A series of 22 compounds of thiazole-5-carboxylic acid derivatives was rationally designed and synthesized. All the compounds were characterized by using ¹H and ¹³C NMR and tested against xanthine oxidase enzyme by spectrophotometric assay. Majority of the compounds were found active against the enzyme amongst which **GK-20** with an IC₅₀ value of 0.45 μM was found to be most potent. Structure-activity relationship obtained from the biological results revealed that the di-substituted compounds as Ring B were more potent than that of mono-substituted derivatives. *Para*-substitution on Ring B is crucial for the xanthine oxidase inhibitory potential. Enzyme kinetic studies further revealed their mixed type inhibition behavior. Moreover, the binding pattern of the most potent compound **GK-20** within the febuxostat binding site of the enzyme was further analyzed by using docking studies which revealed that it sufficiently block the catalytic active site, which prevents the substrate to bind.

Keywords Thiazole derivatives · Xanthine oxidase inhibition · Enzyme kinetics · Molecular modeling

Introduction

Xanthine oxidase (XO) is a form of xanthine oxidoreductase, a versatile molybdoflavoprotein that involved in the metabolism of purines, catalyzing the oxidative

hydroxylation of hypoxanthine, and xanthine to produce uric acid (Stockert et al. 2002; Borges et al. 2002; Hille 2006). It is widely distributed, occurring in milk, kidney, lungs, heart, and vascular endothelium but extremely active in liver and intestine in the human body (Dhiman et al. 2012). The functional aberrations of XO lead to many diseases like gout and oxidative damage to the tissue (White 2018).

Consequently, XO is an intensified target, inhibition of which may result in broad-spectrum chemotherapeutic for gout, cancer, inflammation, and oxidative damage (Stockert et al. 2002; Borges et al. 2002; Hille 2006; Pacher et al. 2006). Allopurinol (**1**) (Fig. 1), a purine analog, was approved by the Food and Drug Administration (1966), which acts as a suicide inhibitor of XO by its active metabolite oxypurinol. Oxypurinol can bind only to the reduced/active form of XO (Borges et al. 2002; Massey et al. 1970; Krakoff 1966). However, due to some reported side effects like Steven–Johnson syndrome, worsening of renal function etc. associated with purine backbone of allopurinol, limits its clinical use and led to a search for nonpurine-based XO inhibitors. (Star and Hochberg 1993; Terkeltaub 1993)

These authors contributed equally: Gurinder Kaur, Jatinder V. Singh

Supplementary information The online version of this article (<https://doi.org/10.1007/s00044-019-02461-y>) contains supplementary material, which is available to authorized users.

- ✉ Preet Mohinder S. Bedi
bedi_preet@yahoo.com
- ✉ Harbinder Singh
singh.harbinder40@gmail.com
- ✉ Sahil Sharma
ss.gq2009@gmail.com

¹ Department of Pharmaceutical Sciences, Guru Nanak Dev University, Amritsar, Punjab 143005, India

² TERI-Deakin Nanobiotechnology Centre, The Energy and Resources Institute, TERI Gram, Gual Pahari, Gurugram, Haryana 122001, India

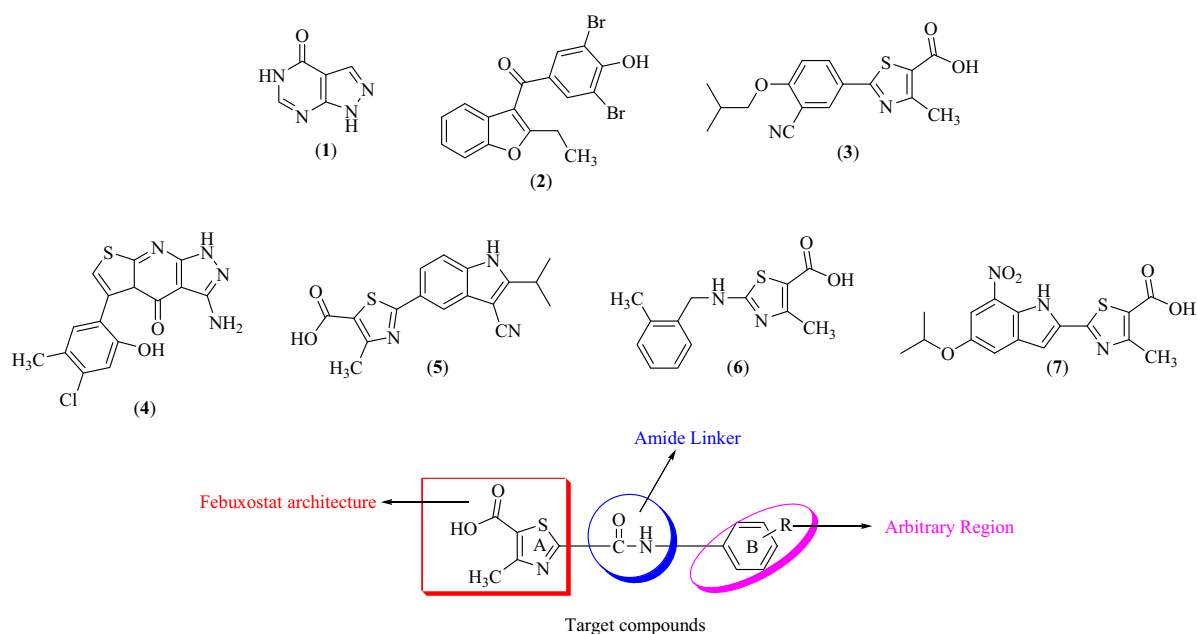


Fig. 1 Reported xanthine oxidase inhibitors and target compounds

In 1970, a nonpurine-based drug named Benzbromarone (2) (Fig. 1) was introduced that promotes the excretion of urate in kidney but not an XO inhibitor itself. Due to its serious hepatotoxicity, it was rapidly withdrawn from the market but still marketed in some European countries (Sinclair and Fox 1975).

After certain efforts, new nonpurine, thiazole containing drug has been introduced in the market named as Febuxostat (3) (Fig. 1), an oral, potent, and selective XO inhibitor with lesser side effects as compared with allopurinol/oxypurinol. It can bind both oxidized and reduced forms of XO (Okamoto et al. 2003; Zhao et al. 2003; Horiuchi et al. 1999). Complete XO inhibition was observed with 25 nM febuxostat, whereas no more than 80% inhibition was seen with either allopurinol or oxypurinol, even at concentrations above those tolerated clinically. The success of this prime, nonpurine XO inhibitor has attracted worldwide attention to develop a structurally diverse array of molecules without purine skeleton.

In similar lines, we are also actively involved in this area for the development of potent nonpurine-based XO inhibitors and have been reported a number of alternate nonpurine molecules in recent past with great potential against XO (Dhiman et al. 2012; Shukla et al. 2014; Sharma et al. 2014; Virdi et al. 2014; Kaur et al. 2015, 2015, 2017; Singh et al. 2014, 2019). Reports on nonpurine thiazole containing XO inhibitors with promising inhibitory potential are also well documented, such as pyrazolo[3,4-*d*]thiazolo[3,2-*a*]pyrimidin-4-one (4) (Khobragade et al. 2010), 2-(3-cyano-2-isopropyl-1H-indol-5-yl)-4-methylthiazole-5-carboxylic acid (5) (Song et al. 2015), 2-(2-methylbenzylamino)-4-

methyl-1,3-thiazole-5-carboxylic acid, (6) (Ali et al. 2016), 2-(7-nitro-5-isopropoxy-indol-2-yl)-4-methylthiazole-5-carboxylic acid (7) (Song et al. 2016). (Fig. 1). With these successive measurements, a new series of thiazole derivatives have been synthesized by keeping intact the thiazole free acid architecture (Ring A) of febuxostat attached with the arbitrary region (Ring B) via amide linker (Fig. 1). Various synthesized analogs were evaluated for their inhibitory potential against XO enzyme using spectrophotometric assay. The type of inhibition and the interactions of the most potent inhibitor within the active site of XO had also been streamlined by using molecular modeling studies.

Experimental

Materials and measurements

The reagents were purchased from Sigma Aldrich, Loba and CDH, India and used without further purification. All yields refer to isolated products after purification. Products were characterized by comparison with authentic samples and by spectroscopic data (^1H and ^{13}C NMR and MASS). ^1H NMR and ^{13}C NMR Spectra were recorded on JEOL AL 300 NMR Spectrometer. The spectra were measured in CDCl_3 relative to TMS (0.00 ppm). In ^1H NMR chemical shifts were reported in δ values using tetramethylsilane as an internal standard with a number of protons, multiplicities (s-singlet, d-doublet, t-triplet, m-multiplet) and coupling constants (*J*) in Hz (Hertz) in the solvent indicated. HRMS was

recorded on microTOF-QII Bruker Daltonik LC-MS/MS High Resolution Mass Spectrometer. Melting points were determined in open capillaries and were uncorrected. Bovine Milk XO of grade I ammonium sulfate suspension was purchased from Sigma Aldrich.

Procedure for synthesis of ethyl 2-amino-4-methylthiazole-5-carboxylate (8)

To a solution of thiourea (0.013 mole) in absolute ethanol (15 mL), 2-chloroethylacetoacetate (1 equivalent) was added dropwise with continuous stirring at room temperature (Ali et al. 2016). After the complete addition of 2-chloroethylacetoacetate, the reaction mixture was warmed on a water bath and the completion of the reaction was monitored by using TLC. After the completion of the reaction, the reaction mixture was cooled at room temperature, the solid crystalline product so obtained was washed with 10 mL of ethanol and then treated with saturated sodium hydrogen carbonate to obtain white precipitates of ethyl 2-amino-4-methylthiazole-5-carboxylate. The characterization data for ethyl 2-amino-4-methylthiazole-5-carboxylate are as follows:

Yield: 90%, mp: 170–174 °C. ^1H NMR (CDCl_3 , 300 MHz, δ , TMS = 0): 4.12 (2H, q, $J = 7.2$ Hz), 2.05 (2H, s), 1.69 (2H, bs), 1.23–1.28 (3H, m) (14-09-2016). ^{13}C NMR (CDCl_3 , 75 MHz, δ , TMS = 0): 16.81, 19.28, 63.26, 160.04, 165.01, 172.14 (28-10-2016). Anal. Calcd. MS: 186.0463; Found m/z : 187.0495 ($\text{M}^+ + 1$). Anal. Calcd. For $\text{C}_7\text{H}_{10}\text{N}_2\text{O}_2\text{S}$: C, 45.15; H, 5.41; N, 15.04; O, 17.18; S, 17.22; Found: C, 45.22; H, 5.35; N, 15.22; S, 17.12.

Procedure for synthesis of ethyl 2-(benzamido)-4-methylthiazole-5-carboxylate derivatives (9)

To a solution of ethyl 2-amino-4-methylthiazole-5-carboxylate (0.005 mole) and pyridine (4 mL), substituted benzoylchlorides (1 equivalent) were added and kept at room temperature for 1 h. Completion of the reaction was monitored by TLC. After the completion of reaction, the reaction mixture was poured on crushed ice, solid mass so obtained was filtered and washed with cold water. The characterization data for ethyl 2-(3,5-difluorobenzamido)-4-methylthiazole-5-carboxylate are as follows:

Yield: 82%, mp: 98–100 °C. ^1H NMR (CDCl_3 , 300 MHz, δ , TMS = 0): 7.50 (2H, d, $J = 6.0$ Hz), 7.05–7.11 (1H, m), 4.34 (2H, q, $J = 7.2$ Hz), 2.59 (3H, s), 1.38 (3H, t, $J = 7.2$ Hz) (3-jan-2017). ^{13}C NMR (CDCl_3 , 75 MHz, δ , TMS = 0): 16.81, 19.28, 63.26, 160.04, 165.01, 172.14 (28-10-2016). Anal. Calcd. MS: 326.0537; Found m/z : 327.0567 ($\text{M}^+ + 1$). Anal. Calcd. For $\text{C}_{14}\text{H}_{12}\text{F}_2\text{N}_2\text{O}_3\text{S}$: C, 51.53; H, 3.71; F, 11.64; N, 8.58; O, 14.71; S, 9.83; Found: C, 51.62; H, 3.66; F, 11.75; N, 8.44; S, 9.99.

Procedure for synthesis of 2-(benzamido)-4-methylthiazole-5-carboxylic acid derivatives (GK-1 to GK-22)

Various substituted derivatives of ethyl 2-(benzamido)-4-methylthiazole-5-carboxylate and potassium carbonate (1 equivalent) were added to a solution of methanol: water (9:1) and refluxed to break the ester into an acid. On completion of the reaction, the reaction mixture was cooled to room temperature and neutralized by adding dropwise glacial acetic acid. Precipitates of desired product so obtained were then filtered, washed with cold water, and recrystallized with ethanol.

Characterization data of all the synthesized compounds are given below:

2-(benzamido)-4-methylthiazole-5-carboxylic acid (GK-1)

Yield 80%, mp 133–136 °C. ^1H NMR (DMSO-d_6 , 300 MHz, δ , TMS = 0): 10.77 (1H, bs), 7.91–7.94 (2H, m), 7.60–7.63 (1H, m), 7.49–7.54 (2H, m), 2.44 (3H, s). ^{13}C NMR (CDCl_3 , 75 MHz, δ , TMS = 0): 20.19, 131.12, 132.13, 132.58, 133.25, 135.08, 136.14, 152.60, 160.02, 162.70, 168.64. Anal. Calcd. MS: 262.0412; Found m/z : 263.0443 ($\text{M}^+ + 1$). Anal. Calcd for $\text{C}_{12}\text{H}_{10}\text{N}_2\text{O}_3\text{S}$: C, 54.95; H, 3.84; N, 10.68; O, 18.30; S, 12.23; Found: C, 54.85; H, 3.92; N, 10.49.

2-(2-fluorobenzamido)-4-methylthiazole-5-carboxylic acid (GK-2)

Yield 77%, mp 170–174 °C. ^1H NMR (DMSO-d_6 , 300 MHz, δ , TMS = 0): 9.96 (1H, bs), 8.20–8.25 (1H, m), 7.61–7.63 (1H, m), 7.20–7.40 (3H, m), 5.32 (1H, s), 2.63 (3H, s). ^{13}C NMR (CDCl_3 , 75 MHz, δ , TMS = 0): 17.52, 125.56, 126.57, 127.64, 158.27, 159.46, 159.94, 163.36, 166.37, 168.54. Anal. Calcd. MS: 280.0318; Found m/z : 281.0349 ($\text{M}^+ + 1$). Anal. Calcd for $\text{C}_{12}\text{H}_9\text{FN}_2\text{O}_3\text{S}$: C, 51.42; H, 3.24; F, 6.78; N, 9.99; O, 17.13; S, 11.44; Found: C, 51.54; H, 3.12; N, 10.05.

2-(3-fluorobenzamido)-4-methylthiazole-5-carboxylic acid (GK-3)

Yield 78%, mp 170–176 °C. ^1H NMR (DMSO-d_6 , 300 MHz, δ , TMS = 0): 10.56 (1H, bs), 7.53–7.70 (2H, m), 7.46–7.51 (1H, m), 7.30–7.35 (1H, m), 2.53 (3H, s). ^{13}C NMR (CDCl_3 , 75 MHz, δ , TMS = 0): 17.41, 125.57, 126.54, 127.63, 158.26, 159.43, 159.96, 163.35, 166.34, 168.55. Anal. Calcd. MS: 280.0318; Found m/z : 281.0350 ($\text{M}^+ + 1$). Anal. Calcd for $\text{C}_{12}\text{H}_9\text{FN}_2\text{O}_3\text{S}$: C, 51.42; H, 3.24; F, 6.78; N, 9.99; O, 17.13; S, 11.44; Found: C, 51.33; H, 3.30; N, 9.93.

2-(4-fluorobenzamido)-4-methylthiazole-5-carboxylic acid (GK-4)

Yield 91%, mp 155–159 °C. ^1H NMR (DMSO-d_6 , 300 MHz, δ , TMS = 0): 10.65 (1H, bs), 8.11 (2H, d, $J = 9.0$ Hz), 7.42 (2H, m), 2.65 (3H, s). ^{13}C NMR (CDCl_3 , 75 MHz, δ , TMS = 0): 17.54, 125.53, 126.58, 127.67, 158.24,

159.42, 159.96, 163.34, 166.33, 168.58. Anal. Calcd. MS: 280.0318; Found *m/z*: 281.0348 ($M^+ + 1$). Anal. Calcd for $C_{12}H_9FN_2O_3S$: C, 51.42; H, 3.24; F, 6.78; N, 9.99; O, 17.13; S, 11.44; Found: C, 51.44; H, 3.18; N, 10.02.

2-(3,5-difluorobenzamido)-4-methylthiazole-5-carboxylic acid (GK-5) Yield 89%, mp 162–168 °C. 1H NMR (DMSO- d_6 , 300 MHz, δ , TMS = 0): 10.58 (1H, bs), 7.50 (2H, d, $J = 6$ Hz), 7.08 (1H, s), 2.58 (3H, s). ^{13}C NMR (CDCl $_3$, 75 MHz, δ , TMS = 0): 17.78, 125.56, 126.52, 127.63, 129.24, 131.68, 145.63, 153.26, 158.23, 159.44, 159.94, 163.35, 168.52. Anal. Calcd. MS: 298.0224; Found *m/z*: 299.0256 ($M^+ + 1$). Anal. Calcd for $C_{12}H_8F_2N_2O_3S$: C, 48.32; H, 2.70; F, 12.74; N, 9.39; O, 16.09; S, 10.75; Found: C, 48.44; H, 2.68; N, 9.46.

2-(3-chlorobenzamido)-4-methylthiazole-5-carboxylic acid (GK-6) Yield 71%, mp 147–151 °C. 1H NMR (DMSO- d_6 , 300 MHz, δ , TMS = 0): 10.56 (1H, bs), 7.50–7.62 (2H, m), 7.46–7.51 (1H, m), 7.28–7.31 (1H, m), 2.51 (3H, s). ^{13}C NMR (CDCl $_3$, 75 MHz, δ , TMS = 0): 17.41, 125.57, 126.54, 127.63, 158.26, 159.43, 159.96, 163.35, 166.34, 168.55. Anal. Calcd. MS: 296.0022; Found *m/z*: 297.97991 ($M^+ + 1$). Anal. Calcd for $C_{12}H_9ClN_2O_3S$: C, 48.57; H, 3.06; Cl, 11.95; N, 9.44; O, 16.18; S, 10.81; Found: C, 48.64; H, 3.01; N, 9.55.

2-(2,3-dichlorobenzamido)-4-methylthiazole-5-carboxylic acid (GK-7) Yield 75%, mp 174–178 °C. 1H NMR (DMSO- d_6 , 300 MHz, δ , TMS = 0): 10.74 (1H, bs), 8.02 (1H, m), 7.62 (1H, m), 7.44 (1H, m), 2.61 (3H, s). ^{13}C NMR (CDCl $_3$, 75 MHz, δ , TMS = 0): 17.85, 125.58, 126.59, 127.65, 133.68, 135.24, 153.26, 158.26, 159.48, 159.95, 163.38, 168.58. Anal. Calcd. MS: 331.9633; Found *m/z*: 331.9601 ($M^+ + 1$). Calcd for $C_{12}H_8Cl_2N_2O_3S$: C, 43.52; H, 2.43; Cl, 21.41; N, 8.46; O, 14.49; S, 9.68; Found: C, 43.66; H, 2.33; N, 8.67.

2-(2-bromobenzamido)-4-methylthiazole-5-carboxylic acid (GK-8) Yield 87%, mp 137–139 °C. 1H NMR (DMSO- d_6 , 300 MHz, δ , TMS = 0): 10.75 (1H, bs), 8.05 (1H, d, $J = 9.0$ Hz), 7.82 (1H, m), 7.65 (1H, m), 7.49 (1H, m), 2.64 (3H, s). ^{13}C NMR (CDCl $_3$, 75 MHz, δ , TMS = 0): 17.80, 121.54, 125.52, 126.53, 127.64, 133.24, 135.68, 158.28, 159.43, 159.96, 163.33, 168.55. Anal. Calcd. MS: 339.9517; Found *m/z*: 341.9495 ($M^+ + 1$). Anal. Calcd for $C_{12}H_9BrN_2O_3S$: C, 42.3; H, 2.66; Br, 23.42; N, 8.21; O, 14.07; S, 9.40; Found: C, 42.35; H, 2.45; N, 8.235.

2-(3-bromobenzamido)-4-methylthiazole-5-carboxylic acid (GK-9) Yield 81%, mp 180–185 °C. 1H NMR (DMSO- d_6 , 300 MHz, δ , TMS = 0): 10.71 (1H, bs), 8.23 (1H, s), 7.93–9.04 (2H, m), 7.55 (1H, m), 2.66 (3H, s). ^{13}C NMR

(CDCl $_3$, 75 MHz, δ , TMS = 0): 17.82, 121.55, 125.57, 126.58, 127.63, 133.25, 135.63, 158.24, 159.46, 159.93, 163.35, 168.58. Anal. Calcd. MS: 339.9517; Found *m/z*: 341.9494 ($M^+ + 1$). Anal. Calcd for $C_{12}H_9BrN_2O_3S$: C, 42.31; H, 2.66; Br, 23.42; N, 8.21; O, 14.07; S, 9.40; Found: C, 42.38; H, 2.42; N, 8.244.

2-(4-bromobenzamido)-4-methylthiazole-5-carboxylic acid (GK-10) Yield 91%, mp 201–203 °C. 1H NMR (DMSO- d_6 , 300 MHz, δ , TMS = 0): 10.76 (1H, bs), 7.99 (2H, d, $J = 8.4$ Hz), 7.77–7.82 (2H, m), 2.63 (3H, s). ^{13}C NMR (CDCl $_3$, 75 MHz, δ , TMS = 0): 17.83, 121.57, 125.53, 126.52, 127.65, 133.23, 135.66, 158.27, 159.43, 159.95, 163.32, 168.53. Anal. Calcd. MS: 339.9517; Found *m/z*: 341.9493 ($M^+ + 1$). Anal. Calcd for $C_{12}H_9BrN_2O_3S$: C, 42.31; H, 2.66; Br, 23.42; N, 8.21; O, 14.07; S, 9.40; Found: C, 42.23; H, 2.56; N, 8.232.

2-(2-iodobenzamido)-4-methylthiazole-5-carboxylic acid (GK-11) Yield 76%, mp 124–130 °C. 1H NMR (DMSO- d_6 , 300 MHz, δ , TMS = 0): 10.71 (1H, bs), 7.65–7.77 (2H, m), 7.38–7.47 (2H, m), 4.83 (1H, bs), 2.36 (3H, s). ^{13}C NMR (CDCl $_3$, 75 MHz, δ , TMS = 0): 17.20, 95.77, 119.03, 131.47, 132.32, 135.75, 142.04, 143.68, 159.12, 163.71, 165.55, 170.13. Anal. Calcd. MS: 387.9379; Found *m/z*: 388.9410 ($M^+ + 1$). Anal. Calcd for $C_{12}H_9IN_2O_3S$: C, 37.13; H, 2.34; I, 32.69; N, 7.22; O, 12.36; S, 8.26; Found: C, 37.24; H, 2.19; N, 7.21.

2-(3-nitrobenzamido)-4-methylthiazole-5-carboxylic acid (GK-12) Yield 84%, mp 180–188 °C. 1H NMR (DMSO- d_6 , 300 MHz, δ , TMS = 0): 10.76 (1H, bs), 9.01 (1H, s), 8.62–7.70 (2H, m), 7.99–8.03 (1H, m), 2.67 (3H, s). ^{13}C NMR (CDCl $_3$, 75 MHz, δ , TMS = 0): 17.79, 121.53, 125.55, 126.56, 133.27, 135.64, 147.73, 158.26, 159.44, 159.97, 163.36, 168.57. Anal. Calcd. MS: 307.0263; Found *m/z*: 308.0294 ($M^+ + 1$). Anal. Calcd for $C_{12}H_9N_3O_5S$: C, 46.90; H, 2.95; N, 13.67; O, 26.03; S, 10.44; Found: C, 46.99; H, 2.88; N, 13.73.

2-(4-nitrobenzamido)-4-methylthiazole-5-carboxylic acid (GK-13) Yield 87%, mp 210–212 °C. 1H NMR (DMSO- d_6 , 300 MHz, δ , TMS = 0): 10.73 (1H, bs), 8.55–8.59 (2H, m), 8.32 (2H, d, $J = 8.4$ Hz), 2.65 (3H, s). ^{13}C NMR (CDCl $_3$, 75 MHz, δ , TMS = 0): 17.80, 121.56, 125.58, 126.55, 133.25, 135.67, 147.78, 158.28, 159.43, 159.96, 163.32, 168.55. Anal. Calcd. MS: 307.0263; Found *m/z*: 308.0293 ($M^+ + 1$). Anal. Calcd for $C_{12}H_9N_3O_5S$: C, 46.90; H, 2.95; N, 13.67; O, 26.03; S, 10.44; Found: C, 47.01; H, 2.81; N, 13.78.

2-(3,5-dinitrobenzamido)-4-methylthiazole-5-carboxylic acid (GK-14) Yield 92%, mp 208–214 °C. 1H NMR (DMSO- d_6 , 300 MHz, δ , TMS = 0): 10.77 (1H, bs), 9.48

(1H, s), 9.177 (1H, s), 7.48 (1H, s), 2.66 (3H, s). ¹³C NMR (CDCl₃, 75 MHz, δ, TMS = 0): 17.20, 95.77, 119.03, 131.47, 132.32, 135.75, 142.04, 143.68, 159.12, 163.71, 165.55, 170.13. Anal. Calcd. MS: 352.0114; Found *m/z*: 353.0145 (M⁺ + 1). Anal. Calcd for C₁₂H₈N₄O₇S: C, 40.91; H, 2.29; N, 15.90; O, 31.79; S, 9.10; Found: C, 40.98; H, 2.34; N, 15.83.

2-(4-methylbenzamido)-4-methylthiazole-5-carboxylic acid (GK-15) Yield 77%, mp 161–164 °C. ¹H NMR (DMSO-d₆, 300 MHz, δ, TMS = 0): 10.77 (1H, bs), 8.00 (2H, d, *J* = 8.0 Hz), 7.35–7.40 (2H, m), 2.63 (3H, s), 2.43 (3H, s). ¹³C NMR (CDCl₃, 75 MHz, δ, TMS = 0): 17.19, 23.45, 120.64, 124.54, 126.65, 132.32, 142.04, 143.68, 159.17, 163.78, 165.54, 170.17. Anal. Calcd. MS: 276.0569; Found *m/z*: 277.0599 (M⁺ + 1). Anal. Calcd for C₁₃H₁₂N₂O₃S: C, 56.51; H, 4.38; N, 10.14; O, 17.37; S, 11.60; Found: C, 56.57; H, 4.24; N, 10.27.

2-(3,5-dimethylbenzamido)-4-methylthiazole-5-carboxylic acid (GK-16) Yield 90%, mp 184–189 °C. ¹H NMR (DMSO-d₆, 300 MHz, δ, TMS = 0): 10.43 (1H, bs), 8.21 (2H, s), 7.45 (1H, m), 2.68 (3H, s), 2.46 (6H, s). ¹³C NMR (CDCl₃, 75 MHz, δ, TMS = 0): 20.19, 120.67, 123.83, 124.57, 126.63, 132.36, 142.03, 143.64, 159.13, 163.73, 165.58, 170.11. Anal. Calcd. MS: 290.0725; Found *m/z*: 291.0757 (M⁺ + 1). Anal. Calcd for C₁₄H₁₄N₂O₃S: C, 57.9; H, 4.86; N, 9.65; O, 16.53; S, 11.04; Found: C, 57.82; H, 4.92; N, 9.61.

2-(2-trifluoromethylbenzamido)-4-methylthiazole-5-carboxylic acid (GK-17) Yield 76%, mp 145–149 °C. ¹H NMR (DMSO-d₆, 300 MHz, δ, TMS = 0): 10.71 (1H, bs), 7.65–7.77 (2H, m), 7.38–7.47 (2H, m), 4.83 (1H, bs), 2.36 (3H, s). ¹³C NMR (CDCl₃, 75 MHz, δ, TMS = 0): 17.20, 95.77, 119.03, 131.47, 132.32, 135.75, 142.04, 143.68, 159.12, 163.71, 165.55, 170.13. Anal. Calcd. MS: 330.286; Found *m/z*: 331.319 (M⁺ + 1). Anal. Calcd for C₁₃H₉F₃N₂O₃S: C, 47.27; H, 2.75; F, 17.26; N, 8.48; O, 14.53; S, 9.71; Found: C, 47.12; H, 2.76; F, 17.23; N, 8.56; S, 9.65.

2-(3-trifluoromethylbenzamido)-4-methylthiazole-5-carboxylic acid (GK-18) Yield 76%, mp 140–142 °C. ¹H NMR (DMSO-d₆, 300 MHz, δ, TMS = 0): 10.45 (1H, bs), 7.34–7.39 (2H, m), 7.28–7.31 (1H, m), 7.22 (1H, s), 2.35 (3H, s). ¹³C NMR (CDCl₃, 75 MHz, δ, TMS = 0): 17.20, 95.77, 119.03, 131.47, 132.32, 135.75, 142.04, 143.68, 159.12, 163.71, 165.55, 170.13. Anal. Calcd. MS: 330.286; Found *m/z*: 331.317 (M⁺ + 1). Anal. Calcd for C₁₃H₉F₃N₂O₃S: C, 47.27; H, 2.75; F, 17.26; N, 8.48; O, 14.53; S, 9.71; Found: C, 47.36; H, 2.45; F, 17.34; N, 8.23; S, 9.76.

2-(4-trifluoromethylbenzamido)-4-methylthiazole-5-carboxylic acid (GK-19) Yield 77%, mp 134–141 °C. ¹H NMR (DMSO-d₆, 300 MHz, δ, TMS = 0): 10.74 (1H, bs), 8.21 (2H, d, *J* = 8.0 Hz), 7.78–7.83 (2H, m), 2.43 (3H, s). ¹³C NMR (CDCl₃, 75 MHz, δ, TMS = 0): 17.19, 23.45, 120.64, 124.54, 126.65, 132.32, 142.04, 143.68, 159.17, 163.78, 165.54, 170.17. Anal. Calcd. MS: 330.286; Found *m/z*: 331.318 (M⁺ + 1). Anal. Calcd for C₁₃H₉F₃N₂O₃S: C, 47.27; H, 2.75; F, 17.26; N, 8.48; O, 14.53; S, 9.71; Found: C, 47.32; H, 2.56; F, 17.45; N, 8.32; S, 9.56.

2-(3,5-difluoromethylbenzamido)-4-methylthiazole-5-carboxylic acid (GK-20) Yield 91%, mp 182–190 °C. ¹H NMR (DMSO-d₆, 300 MHz, δ, TMS = 0): 10.76 (1H, bs), 8.22–8.27 (2H, m), 7.98 (1H, m), 2.74 (3H, s). ¹³C NMR (CDCl₃, 75 MHz, δ, TMS = 0): 18.85 (thiazole-CH3), 125.56, 126.52, 127.63, 129.24, 131.68, 145.63, 153.26, 158.23, 159.44, 159.94, 163.35 (CONH), 168.52 (C–O). Anal. Calcd. MS: 398.0160; Found *m/z*: 399.0190 (M⁺ + 1). Anal. Calcd for C₁₄H₈F₆N₂O₃S: C, 42.22; H, 2.02; F, 28.62; N, 7.03; O, 12.05; S, 8.05; Found: C, 42.27; H, 1.98; F, 28.74; N, 6.99; S, 8.12.

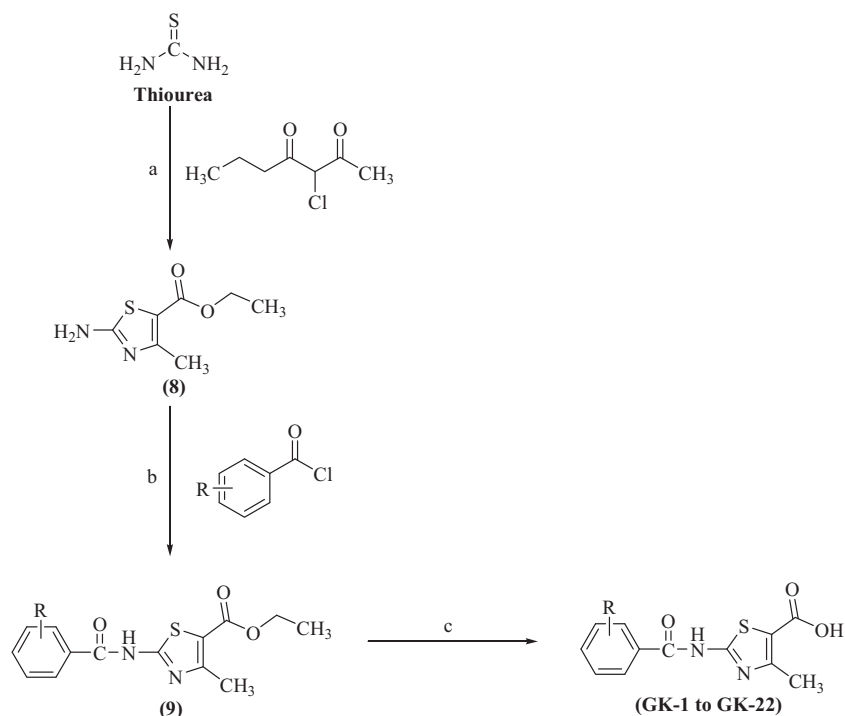
2-(4-methoxybenzamido)-4-methylthiazole-5-carboxylic acid (GK-21) Yield 91%, mp 157–162 °C. ¹H NMR (DMSO-d₆, 300 MHz, δ, TMS = 0): 10.71 (1H, bs), 8.17 (2H, d, *J* = 8.5 Hz), 7.11 (2H, d, *J* = 8.5 Hz), 3.61 (3H, s), 2.62 (3H, s). ¹³C NMR (CDCl₃, 75 MHz, δ, TMS = 0): 17.34, 60.34, 125.59, 126.56, 127.62, 153.22, 158.21, 159.46, 159.93, 163.37, 165.34, 168.54. Anal. Calcd. MS: 292.0518; Found *m/z*: 293.0549 (M⁺ + 1). Anal. Calcd for C₁₃H₁₂N₂O₄S: C, 53.42; H, 4.14; N, 9.58; O, 21.89; S, 10.97; Found: C, 53.34; H, 4.19; N, 9.51.

2-(3,4-dimethoxybenzamido)-4-methylthiazole-5-carboxylic acid (GK-22) Yield 91%, mp 143–145 °C. ¹H NMR (DMSO-d₆, 300 MHz, δ, TMS = 0): 10.71 (1H, bs), 8.19 (1H, s), 7.23–7.31 (2H, m), 3.61 (3H, s), 2.65 (6H, s). ¹³C NMR (CDCl₃, 75 MHz, δ, TMS = 0): 17.34, 60.34, 125.59, 126.56, 127.62, 153.22, 158.21, 159.46, 159.93, 163.37, 165.34, 168.54. Anal. Calcd. MS: 322.0623; Found *m/z*: 323.0655 (M⁺ + 1). Anal. Calcd for C₁₄H₁₄N₂O₅S: C, 52.17; H, 4.38; N, 8.69; O, 24.82; S, 9.95; Found: C, 52.34; H, 4.16; N, 8.84; S, 9.76.

In vitro xanthine oxidase assay

All the synthesized compounds were evaluated against XO enzyme. Bovine milk XO (grade 1, ammonium sulfate suspension, Sigma-Aldrich) activity was assayed spectrophotometrically by measuring the uric acid formation at 293 nm using a Hitachi U-3010 UV-visible spectrophotometer at 25 °C. The reaction mixture contains

Scheme 1 Synthesis of thiazole derivatives. Reagents and conditions: **a** Ethanol, reflux, 70 °C; **b** pyridine, stirring rt, 1 h; **c** methanol: water (9:1), K₂CO₃, stirring with reflux



potassium phosphate buffer (pH 7.6, 50 Mm, 100 μ L), xanthine (75 μ M, 20 μ L), and XO (0.08 units). Inhibition of XO activity of synthetics at different concentrations (1, 5, 10, 25, 50 μ M) was measured by following the decrease in the uric acid formation at 293 nm at 25 °C. The enzyme was preincubated for 5 min with a test compounds, dissolved in DMSO (1% v/v), and the reaction was started by the addition of xanthine. The final concentration of DMSO (1% v/v) did not interfere with the enzyme activity. All the experiments were performed in triplicate and values were expressed as the mean of three experiments (Escribano et al. 1988; Takano et al. 2005).

Enzyme kinetics

Potent XO enzyme inhibitors were further investigated for the type of inhibition and enzyme kinetics study was carried out. The Lineweaver–Burk plot was established from which we could calculate the K_m , V_{max} of the slope of inhibitor and the value of α (a constant that defines the degree to which inhibitor binding affects the affinity of the enzyme for substrate) (Copeland 2005).

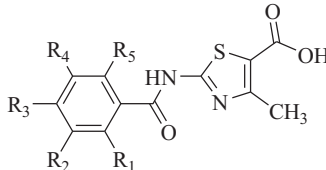
Molecular modeling studies

Three-dimensional structure of bovine milk xanthine dehydrogenase complexed with fabuxostat (a potent XO inhibitor) was retrieved from RCSB protein data bank (PDB code 1N5X) (Okamoto et al. 2003). For docking simulations, hydrogens were added onto the protein structure

using MGL Tools-1.5.6. Two-dimensional structure of ligand **GK-20** was drawn in ChemDraw and subjected to energy minimization using the MM2 force field as implemented in Chem 3D Ultra software (Cambridge, USA) Docking of **GK-20** was performed using the AutoDock Vina software (Trott and Olson 2010). For docking performance, a grid box was generated by fixing the number of points in x, y, and z directions to 40, each. The spacing was adjusted to 1.00 Å. The center of the grid box was fixed to the point of 96, 52, and 38.

Results and discussion

Thiazole-5-carboxylic acid derivatives were synthesized via Scheme 1. To a mixture of thiourea (0.013 moles) and ethanol (15 mL), 2-chloroethylacetoacetate (1 equivalent) was added dropwise with continuous stirring at room temperature. After the complete addition of 2-chloroethylacetoacetate, the reaction mixture was warmed on a water bath and the completion of the reaction was monitored by using TLC. After completion, the reaction mixture was cooled at room temperature and solid crystalline product so obtained was washed with 10 mL of ethanol and then treated with saturated sodium hydrogen carbonate to obtain white precipitates of ethyl 2-amino-4-methylthiazole-5-carboxylate (Ali et al. 2016). Thiazole derivative was further subjected to benzoylation using various benzoylchlorides in presence of dry pyridine at room temperature. This product was further hydrolyzed by using

Table 1 Various substituted thiazole-5-carboxylic acid derivatives


Code	R ₁	R ₂	R ₃	R ₄	R ₅	mp (°C)
GK-1	H	H	H	H	H	132–136
GK-2	F	H	H	H	H	170–174
GK-3	H	F	H	H	H	170–176
GK-4	H	H	F	H	H	155–159
GK-5	H	F	H	F	H	162–168
GK-6	H	Cl	H	H	H	147–151
GK-7	Cl	Cl	H	H	H	174–178
GK-8	Br	H	H	H	H	137–139
GK-9	H	Br	H	H	H	180–185
GK-10	H	H	Br	H	H	201–203
GK-11	I	H	H	H	H	124–130
GK-12	H	NO ₂	H	H	H	180–188
GK-13	H	H	NO ₂	H	H	210–212
GK-14	H	NO ₂	H	NO ₂	H	208–214
GK-15	H	H	CH ₃	H	H	161–164
GK-16	H	CH ₃	H	CH ₃	H	184–189
GK-17	CF ₃	H	H	H	H	145–149
GK-18	H	CF ₃	H	H	H	140–142
GK-19	H	H	CF ₃	H	H	134–141
GK-20	H	CF ₃	H	CF ₃	H	182–190
GK-21	H	H	OCH ₃	H	H	157–162
GK-22	H	OCH ₃	OCH ₃	H	H	143–145

potassium carbonate in the presence of methanol: water (9:1) to obtain the target compounds. All the reactions proceeded smoothly with diverse benzoylchlorides and products were obtained in good yields (Table 1). The structures of the synthesized compounds were elucidated by ¹H and ¹³C NMR. All spectral data were in accordance with assumed structures.

In vitro biological evaluation

For in vitro screening of the thiazole-5-carboxylic acid derivatives, enzymatic assay using bovine milk XO (grade 1, ammonium sulfate suspension) was performed as described in the literature (Escrignano et al. 1988; Takano et al. 2005). Febuxostat and allopurinol were employed as reference inhibitors (Escrignano et al. 1988; Takano et al. 2005). The results of the in vitro assay (Table 2) indicated that the derivatives exhibited significant XO inhibitory activity amongst which the most potent compound (**GK-20**)

Table 2 Percentage inhibition and IC₅₀ values of thiazole-5-carboxylic acid derivatives against XO

Compound	Percent inhibition					IC ₅₀ (μM ± SD)
	1 μM	5 μM	10 μM	25 μM	50 μM	
GK-1	15	28	38	57	69	14.70 ± 1.03
GK-2	13	24	36	48	61	29.14 ± 2.44
GK-3	28	33	43	54	68	13.88 ± 2.09
GK-4	51	58	64	71	83	0.75 ± 0.09
GK-5	53	58	69	72	86	0.53 ± 0.08
GK-6	18	24	39	55	67	23.45 ± 2.33
GK-7	52	59	67	72	89	0.71 ± 0.05
GK-8	5	9	14	18	24	ND
GK-9	7	11	14	17	19	ND
GK-10	11	16	23	29	32	ND
GK-11	4	5	8	11	15	ND
GK-12	15	21	29	33	40	ND
GK-13	18	21	30	36	43	ND
GK-14	10	22	32	41	55	44.45 ± 3.56
GK-15	44	53	60	69	75	4.01 ± 0.46
GK-16	47	57	66	72	78	2.44 ± 0.32
GK-17	41	48	56	63	69	8.11 ± 0.86
GK-18	22	31	38	49	55	ND
GK-19	43	51	59	69	71	5.05 ± 0.87
GK-20	55	63	76	87	98	0.45 ± 0.03
GK-21	31	38	45	56	62	12.55 ± 0.81
GK-22	40	48	54	60	69	8.40 ± 0.97
Febuxostat						0.03
Allopurinol						8.69

The bold values provided of standard drugs, provided to compare the biological results with synthesized compounds

showed 98% inhibition at 50 μM concentration. The concentration to inhibit the 50% of the enzyme (IC₅₀) was only calculated for those compounds, which displayed more than 60% inhibition at 50 μM concentration. The obtained IC₅₀ values were ranging from 0.45–44.45 μM. Nine compounds (**GK-4**, **GK-5**, **GK-7**, **GK-15** to **GK-17**, **GK-19**, **GK-20**, and **GK-22**) were found more potent than standard drug allopurinol (IC₅₀ = 8.69 μM). The most potent compound (**GK-20**) was endowed with the most potent inhibitory activity with the IC₅₀ value of 0.45 μM, which was found almost 20 times more potent than allopurinol. **GK-4**, **GK-5**, and **GK-7** are other potent compounds of the series with the IC₅₀ values of 0.75, 0.53, and 0.71 μM, respectively. The in vitro screening of the thiazole-5-carboxylic acid derivatives revealed some interesting aspects of the structure-activity relationship. Unsubstituted Ring B showed moderate inhibitory activity against the enzyme. Careful examination of the biological data (Table 2) indicates that mono-substituted compounds (as Ring B) are less active than di-substituted compounds (compare **GK-4** with **GK-5**, **GK-6** with **GK-7**,

GK-13 with **GK-14**, **GK-15** with **GK-16**, **GK-19** with **GK-20**, and **GK-21** with **GK-22**). It has also been cleared from the evaluation results that *para* position of Ring B for halogen atoms is more sensitive towards the XO inhibitory activity. It means that compounds with halogen atoms on *para* position of Ring B were found more active than *ortho* and *meta* halogenated compounds (compare **GK-4** and **GK-20** with **GK-2**, **GK-3**, **GK-6**, and **GK-11**).

Enzyme kinetics

The most potent XO inhibitor among the series (**GK-20**) was further investigated for the type of inhibition by enzyme kinetic studies. The reactions were performed at different concentrations of inhibitor **GK-20** (at 1, 10 and 50 μM). The pattern of the Lineweaver–Burk plot indicates that it inhibited the enzyme by mixed type inhibition scenario, where K_m , V_{max} , and slope are all affected by the inhibitor. (Fig. 2) The inhibitor has increased the K_m and slope (K_m/V_{max}) while decreasing the V_{max} . Moreover, on careful observation, it was found that intersecting lines on the graph converge to the left of the y -axis and above the x -axis, which indicates that the value of α (affinity constant) is >1 (Copeland 2005). This confirms that the inhibitor preferentially binds to the free enzyme and not the enzyme–substrate complex.

Molecular modeling studies

In order to understand the binding conformation of inhibitors, the most potent XO inhibitor **GK-20** was docked into the februxostat binding site using the AutoDock Vina software (Fig. 3). Docking procedure was validated by reproducing co-crystallized conformation of februxostat. The AutoDock Vina was able to reproduce the co-crystallized conformation of februxostat with the RMSD value of 0.792 Å (Fig. 3a), which ensures the acceptability of the selected docking protocol. Several docked conformations of

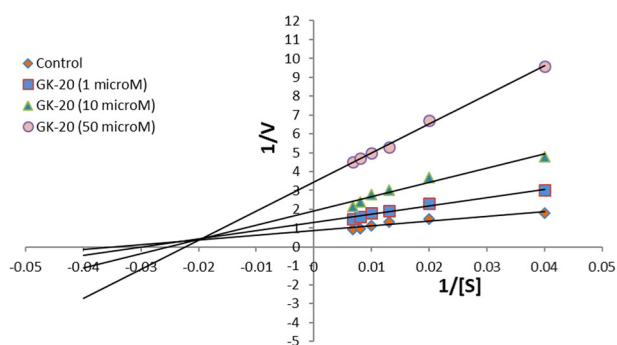


Fig. 2 Lineweaver–Burk plot of compound **GK-20**

GK-20 were generated and ranked according to their *in silico* binding affinity. The conformation with a highest binding affinity (-8.7 kcal/mol) was selected for discussion (Fig. 3a, b).

The Two-dimensional depiction of various residues surrounding **GK-20** is presented in Fig. 3b. The binding site residues and overall binding mode of **GK-20** is similar to those observed with februxostat (Okamoto et al. 2003), salicylic acid (Enroth et al. 2000), and curcumin (Shen and Ji 2009). **GK-20** gets stabilized at the binding cavity by various electrostatic interactions. The major interactions include two π – π stacking and three H-bond interactions (Fig. 3c). The thiazole ring gets sandwiched between Phe914 and Phe1009 and involved in *face-to-face* and *edge-to-face* π – π stacking interactions, respectively ($d = 4.387$ Å and 3.430 Å). This arrangement of energetically favorable π – π stacking interactions has also seen in the co-crystal structure of XO with februxostat and salicylate (Okamoto et al. 2003; Enroth et al. 2000). Its conservation argues for an important role in stabilizing the binding positions of aromatic substrates and it might well represent one of the key features of substrate recognition. The carboxylate function at thiazole ring (H-bond acceptor) has shown two H-bond interactions with strongly basic guanidine group of Arg880 (H-bond donor; $d = 2.225$ Å and 2.537 Å). H-bond interaction observed between carbonyl function of amide linker chain (H-acceptor) and the hydroxyl group of Ser876 (H-bond donor; $d = 2.051$ Å) makes it a suitable confirmation similarly as seen in previously designed lead molecules (Ali et al. 2016). The 3,5-di-substituted phenyl ring gets positioned in a cavity formed by Leu648, Phe649, Leu873, Val1011, Leu1014, and Lys771 and stabilized by van der Waals and/or dispersion interactions. The study suggests that **GK-20** may block the activity of the XO sufficiently enough to prevent the substrate from binding to its active site.

In silico study

Furthermore, to confirm that whether the compounds can be used for animal studies, *in silico* physicochemical properties of active compounds were determined by using the web-based applications MarvinSketch (<http://www.chemaxon.com/>) and PreADMET (<http://preadmet.bmdrc.org/>). Table 3 indicated that the compounds are predicted to have lower blood–brain barrier permeation which suggests that they are found less likely to cause neurotoxicity. Parameters of the Lipinski rule of five of all the synthesized compounds were determined with ChemAxon software MarvinSketch (Table 4). Tabular values indicate that all the molecules have a molecular weight in the range of 262–398 which lies in the limit of 180–500. Compounds have no H-bond donating

Fig. 3 **a** Superimposition of co-crystallized (green) and docked conformation (magenta) of febuxostat (RMSD: 0.792 Å); **b**. Two-dimensional representation of **GK-20** at febuxostat binding site; **c**. Three-dimensional Docking conformation of **GK-20** (Hydrogens which are involved in H-bond interactions are shown)

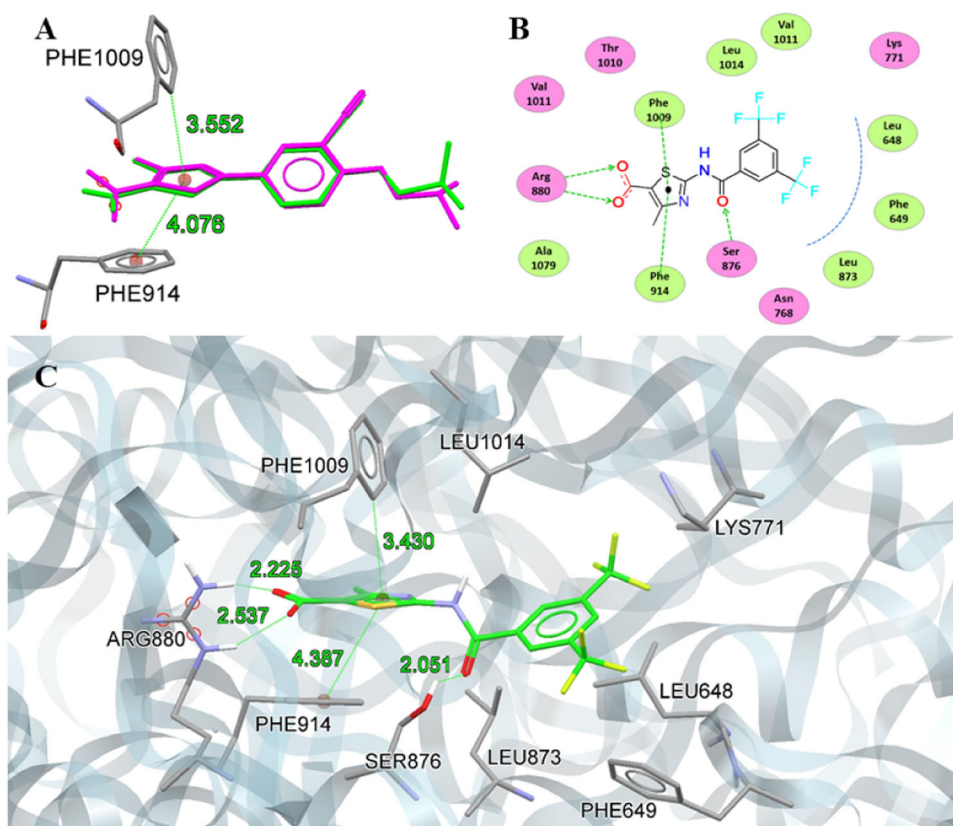


Table 3 In silico ADME properties of active compounds

Compound	Absorption				Distribution	
	Human intestinal absorption (HIA)%	In vitro Caco-2 cell permeability (nm/s)	In vitro MDCK cell permeability (nm/s)	In vitro skin permeability (logKp) cm/h	In vitro plasma protein binding (%)	In vivo blood–brain barrier penetration (C. brain/C.blood)
<i>GK-1</i>	89.13	1.02	40.10	−3.79	62.56	0.30
<i>GK-2</i>	89.24	0.91	43.06	−4.06	72.61	0.35
<i>GK-3</i>	89.24	0.91	37.45	−4.06	71.65	0.35
<i>GK-4</i>	89.24	10.05	42.20	−4.04	70.66	0.03
<i>GK-5</i>	89.34	0.84	34.10	−4.21	78.04	0.40
<i>GK-6</i>	94.49	4.39	20.06	−3.87	73.66	0.49
<i>GK-7</i>	97.11	4.28	3.84	−3.82	83.55	0.82
<i>GK-14</i>	13.28	1.10	9.89	−3.79	87.32	0.04
<i>GK-15</i>	90.52	0.87	28.13	−3.71	70.81	0.43
<i>GK-16</i>	91.75	3.16	27.45	−3.70	80.46	0.16
<i>GK-17</i>	90.80	1.19	20.70	−2.68	81.82	0.66
<i>GK-19</i>	90.80	0.89	0.06	−2.71	75.94	0.18
<i>GK-20</i>	92.23	30.00	0.04	−2.10	96.73	0.01
<i>GK-21</i>	86.61	3.65	23.66	−3.99	67.70	0.09
<i>GK-22</i>	83.68	2.81	2.87	−4.15	66.62	0.11

and accepting properties within the described limits. Molar refractivities are consistent and lie well in the range of 40–130. From the log *P* values, it has been cleared that the

compounds are not very lipophilic in nature. These results make the compounds pharmacologically efficient for use in the animal model.

Table 4 Physicochemical parameters of active compounds

Compound	Molecular weight	No. of H-bond donors	No. of H-bond acceptors	Molar refractivity	Log <i>P</i>	No. of Lipinski violation
<i>GK-1</i>	262	2	4	67.91	2.33	0
<i>GK-2</i>	280	2	4	68.12	2.47	0
<i>GK-3</i>	280	2	4	68.12	2.47	0
<i>GK-4</i>	280	2	4	68.12	2.47	0
<i>GK-5</i>	298	2	4	68.34	2.61	0
<i>GK-6</i>	296	2	4	72.71	2.93	0
<i>GK-7</i>	329	2	4	77.51	3.54	0
<i>GK-14</i>	352	2	8	82.55	2.21	0
<i>GK-15</i>	276	2	4	72.95	2.84	0
<i>GK-16</i>	290	2	4	77.99	3.36	0
<i>GK-17</i>	330	2	4	73.88	3.21	0
<i>GK-19</i>	330	2	4	73.88	3.21	0
<i>GK-20</i>	398	2	4	79.85	4.09	0
<i>GK-21</i>	292	2	5	74.37	2.17	0
<i>GK-22</i>	322	2	6	80.83	2.01	0

Conclusion

A novel series of thiazole-5-carboxylic acid derivatives was synthesized and in vitro evaluated against XO enzyme. Compounds were found significantly active against the enzyme and exhibited the IC₅₀ values ranging from 0.45 to 44.45 μM. The compound **GK-20** was found to be the most potent compound with 3,5-di(trifluoromethyl) substitution on Ring B, which exhibited almost 20 folds potent inhibition (IC₅₀ = 0.45 μM) against the enzyme than allopurinol. The established structure-activity relationship revealed that di-substituted compounds as Ring B were more potent than that of mono-substituted compounds. The *para*-substitution was found to be the most preferable one for the inhibitory potential, other than *ortho*- and *meta*-substitution. Mixed type inhibition scenario was observed for the compound **GK-20** through enzyme kinetic studies. Various types of the binding interactions within the active site of XO enzyme were also streamlined by using docking studies. Thus the compounds could act as hit lead for the further development of potent XO inhibitors.

Acknowledgements Authors are grateful to the University Grants Commission for providing funds under Rajiv Gandhi National Fellowship (RGNF), National Fellowship for Other Backward Classes (NFOBC) and are thankful to Council of Scientific & Industrial Research (CSIR) for providing financial assistance to carry out the research work.

Compliance with ethical standards

Conflict of interest The authors declare that they have no conflict of interest.

Publisher's note Springer Nature remains neutral with regard to jurisdictional claims in published maps and institutional affiliations.

References

- Ali MR, Kumar S, Afzal O, Shalmali N, Sharma M, Bawa S (2016) Development of 2-(substituted benzylamino)-4-methyl-1, 3-thiazole-5-carboxylic acid derivatives as xanthine oxidase inhibitors and free radical scavengers. *Chem Biol Drug Des* 87:508–516
- Borges F, Fernandes E, Roleira F (2002) Progress towards the discovery of xanthine oxidase inhibitors. *Curr Med Chem* 9:195–217
- Copeland RA (2005) *Evaluation of Enzyme Inhibitors in Drug Discovery*. Wiley, Hoboken
- Dhiman R, Sharma S, Singh G, Nepali K, Bedi PMS (2012) Design and synthesis of aza-flavones as a new class of xanthine oxidase inhibitors. *Arch Pharm Chem Life Sci* 346:7–16
- Enroth C, Eger BT, Okamoto K, Nishino T, Nishino T, Pai EF (2000) Crystal structures of bovine milk xanthine dehydrogenase and xanthine oxidase: structure-based mechanism of conversion. *Proc Natl Acad Sci USA* 97:10723–10728
- Escribano J, Gracia-Canovas F, Garcia-Carmona F (1988) A kinetic study of hypoxanthine oxidation by milk xanthine oxidase. *Biochem J* 254:829–833
- Hille R (2006) Structure and function of xanthine oxidoreductase. *Eur J Inorg Chem* 2006:1913–1926
- Horiuchi H, Ota M, Kobayashi M, Kaneko H, Kasahara Y, Nishimura S, Kondo S, Komoriya K (1999) A comparative study on the hypouricemic activity and potency in renal xanthine calculus formation of two xanthine oxidase/xanthine dehydrogenase inhibitors: TEI-6720 and allopurinol in rats. *Res Commun Mol Pathol Pharm* 104:307–319
- Kaur C, Dhiman S, Singh H, Kaur M, Bhagat S, Gupta M, Sharma S, Bedi PMS (2015) Synthesis, screening and docking studies of benzochromone derivatives as xanthine oxidase inhibitors. *J Chem Pharm Res* 7:127–136
- Kaur M, Kaur A, Mankotia S, Singh H, Singh A, Singh JV, Gupta MK, Sharma S, Nepali K, Bedi PMS (2017) Synthesis, screening

- and docking of fused pyrano[3,2-d]pyrimidine derivatives as xanthine oxidase inhibitor. *Eur J Med Chem* 131:14–28
- Kaur R, Naaz F, Sharma S, Mehndiratta S, Gupta MK, Bedi PMS, Nepali K (2015) Screening of a library of 4-aryl/heteroaryl-4H-fused pyrans for xanthine oxidase inhibition: synthesis, biological evaluation and docking studies. (2015). *Med Chem Res* 24:3334–3349
- Khobragade CN, Bodade RG, Dawane BS, Konda SG, Khandare NT (2010) Synthesis and biological activity of pyrazolo[3,4-d]thiazolo[3,2-a]pyrimidin-4-one derivatives: in silico approach. *J Enzym Inhib Med Chem* 25:615–621
- Krakoff IH (1966) Use of allopurinol in preventing hyperuricemia in leukemia and lymphoma. *Cancer* 19:1489–1496
- Massey V, Komai H, Palmer G (1970) On the mechanism of inactivation of xanthine oxidase by allopurinol and other pyrazolo[3,4-d]pyrimidines. *J Bio Chem* 245:2837–2844
- Okamoto K, Eger BT, Nishino T, Kondo S, Pai EF, Nishino T (2003) An extremely potent inhibitor of xanthine oxidoreductase. *J Biol Chem* 278:1848–1855
- Pacher P, Nivorozhkin A, Szabo C (2006) Therapeutic effects of xanthine oxidase inhibitors: renaissance half a century after the discovery of allopurinol. *Pharm Rev* 58:87–114
- Sharma S, Sharma K, Ojha R, Kumar D, Singh G, Nepali K, Bedi PMS (2014) Microwave assisted synthesis of naphthopyrans catalysed by silica supported fluoroboric acid as a new class of non purine xanthine oxidase inhibitors. *Bioorg Med Chem Lett* 24:495–500
- Shen L, Ji HF (2009) Insights into the inhibition of xanthine oxidase by curcumin. *Bioorg Med Chem Lett* 19:5990–5993
- Shukla S, Kumar D, Ojha R, Gupta MK, Nepali K, Bedi PMS (2014) 4,6-diaryl/heteroarylpyrimidin-2(1H)-ones as a new class of xanthine oxidase inhibitors. *Arch Pharm Chem Life Sci* 347:486–495
- Sinclair DS, Fox IH (1975) The pharmacology of hypouricemic effect of benzbromarone. *J Rheumatol* 2:437–445
- Singh H, Sharma S, Ojha R, Gupta MK, Nepali K, Bedi PMS (2014) Synthesis and evaluation of naphthoflavones as a new class of non purine xanthine oxidase inhibitors. *Bioorg Med Chem Lett* 24:4192–4197
- Singh JV, Mal G, Kaur G, Gupta MK, Singh A, Nepali K, Singh H, Sharma S, Bedi PMS (2019) Benzoflavone derivatives as potent antihyperuricemic agents. *Med Chem Commun* 10:128–147
- Song JU, Choi SP, Kim TH, Jung C, Lee J, Kim GT, Jung S (2015) Design and synthesis of novel 2-(indol-5-yl)thiazole derivatives as xanthine oxidase inhibitors. *Bioorg Med Chem Lett* 25:1254–1258
- Song JU, Jang JW, Kim TH, Park H, Park WS, Jung SH, Kim GT (2016) Structure-based design and biological evaluation of novel 2-(indol-2-yl) thiazole derivatives as xanthine oxidase inhibitors. *Bioorg Med Chem Lett* 26:950–954
- Star VL, Hochberg MC (1993) Prevention and management of gout. *Drugs* 45:212–222
- Stockert AL, Shinde SS, Anderson RF, Hille RJ (2002) The reaction mechanism of xanthine oxidase: evidence for two-electron chemistry rather than sequential one-electron steps. *J Am Chem Soc* 124:14554–14555
- Takano Y, Hase-Aoki K, Horiuchi H, Zhao L, Kasahara Y, Kondo S, Becker MA (2005) Selectivity of febuxostat, a novel non-purine inhibitor of xanthine oxidase/xanthine dehydrogenase. *Life Sci* 76:1835–1847
- Terkeltaub RA (1993) Gout and mechanisms of crystal-induced inflammation. *Curr Opin Rheumatol* 5:510–516
- Trott O, Olson AJ (2010) AutoDock Vina: improving the speed and accuracy of docking with a new scoring function, efficient optimization, and multithreading. *J Comput Chem* 31:455–461
- Virdi HS, Sharma S, Mehndiratta S, Bedi PMS, Nepali K (2014) Design, synthesis and evaluation of 2,4-diarylpyrano[3,2-c]chromen-5(4H)-one as a new class of non-purine xanthine oxidase inhibitors *J Enzym Inhib Med Chem* 30:1–7
- White WB (2018) Gout, xanthine oxidase inhibition, and cardiovascular outcomes. *Circulation* 138:1127–1129
- Zhao L, Takano Y, Horiuchi H (2003) Effect of febuxostat, a novel non-purine, selective inhibitor of xanthine oxidase (NP-SIXO), on enzymes in purine and pyrimidine metabolism pathway [abstract]. *Arthritis Rheum* 48:Suppl S531